Characterization of a superconducting Pb photocathode in a superconducting rf photoinjector cavity

R. Barday,* A. Burrill, A. Jankowiak, T. Kamps, J. Knobloch, O. Kugeler, A. Matveenko, A. Neumann, M. Schmeißer, and J. Völker
Helmholtz-Zentrum Berlin für Materialien und Energie GmbH, Hahn-Meitner-Platz 1, 14109 Berlin, Germany

P. Kneisel
Thomas Jefferson National Accelerator Facility, Newport News, Virginia 23606, USA

R. Nietubyc
National Centre for Nuclear Research, Soltana 7, 05-400 Otwock, Poland

S. Schubert and J. Smedley
Brookhaven National Laboratory, Upton, New York 11973, USA

J. Sekutowicz
DESY, Notkestraße 85, 22603 Hamburg, Germany

I. Will
Max-Born-Institut, Max-Born-Straße 2A, 12489 Berlin, Germany
(Received 12 August 2013; published 6 December 2013)

Photocathodes are a limiting factor for the next generation of ultrahigh brightness photoinjectors. We studied the behavior of a superconducting Pb cathode in the cryogenic environment of a superconducting rf gun cavity to measure the quantum efficiency, its spatial distribution, and the work function. We will also discuss how the cathode surface contaminants modify the performance of the photocathode as well as the gun cavity and we discuss the possibilities to remove these contaminants.

DOI: 10.1103/PhysRevSTAB.16.123402 PACS numbers: 85.60.Ha, 79.20.Ds, 41.60.Cr, 07.77.Ka

I. INTRODUCTION

Superconducting radio-frequency (SRF) gun cavities are well suited for the production of a high brightness electron beam with high average current, low beam emittance, and long cathode lifetime [1]. In contrast to normal conducting guns, low rf power losses in the SRF guns allow an operation in a continuous wave (CW) mode at high field gradient on the cathode surface, which allows production of an electron beam with high average current and low beam emittance. The cryogenic environment of the gun cavity provides excellent vacuum conditions needed for a long cathode lifetime. The implementation of a photocathode with high quantum efficiency (QE) and low contribution to the dark current in a way preserving the quality factor of the SRF cavity prior to the cathode deposition is one of the main challenges of the development of SRF electron guns. In addition, any normal conducting photocathode must be thermally isolated from the cavity and mounted in a way that minimizes rf losses in the cathode holder. One solution to this issue has been developed at Helmholtz-Zentrum Dresden-Rossendorf. In this design a normal conducting cathode is deposited on a normal conducting cathode plug, which is isolated from the superconducting cavity by a vacuum gap and is cooled down with liquid nitrogen [2]. A choke filter prevents rf losses downstream the cathode. Another option to integrate a photocathode into an SRF gun is to use a superconducting cathode. In the most simple setup, the back wall of the superconducting Nb cavity can be used as a photoemitter [3]. The major advantage of this solution is a possibility to avoid contaminations of the cavity and to preserve an excellent cathode surface, typical for superconducting cavities. The main disadvantage of the Nb cathode is its high work function ~4.3 eV [4] and low QE $\sim 10^{-5}$ at 258 nm [5]. Alternatively, Nb can be coated with a superconductor having higher QE. The only viable candidate is a lead photocathode as the other superconductors are either highly reactive or have too low critical temperature T_c [1,6]. Lead is a superconductor with $T_c = 7.2$ K and a critical magnetic field of 80 mT compared to Nb which has a T_c of 9.2 K and a critical magnetic field of 200 mT [7]. The QE of clean Pb is a factor of 30 higher than that of Nb at 258 nm [5]. The work function of lead ~4 eV [8] is

*roman.barday@helmholtz-berlin.de

slightly lower than that of niobium. Nevertheless, lead photocathode requires an ultraviolet (UV) drive laser. To achieve this wavelength an infrared laser must be converted to UV by using nonlinear crystals. The conversion process limits the available average power to few Watts. With the present state-of-the-art laser technology the average beam current is limited to a maximum of few hundred μA, preventing the use of the Pb for high average current applications. Nevertheless, an SRF gun with a Pb cathode is suitable for low average current FEL applications, like a possible CW upgrade of the European x-ray free-electron laser (XFEL). Prior to our research, the use of a lead photocathode had been restricted to witness sample measurements at 300 and 80 K only with no measurement data at 2 K, where the cathode is a superconductor [5]. During these bench measurements it was shown that lead photocathodes are less sensitive to gas contaminations than high QE semiconductor photocathodes such as GaAs or CsK_2Sb. Nevertheless, Pb cathodes can be contaminated during transport in air and by a reaction with residual gases, which decreases the cathode QE. For normal conducting metal photocathodes laser cleaning is a well established technique used to remove the contaminations and restore the cathode QE in the normal conducting photoinjectors [9,10]. Here we report on laser cleaning of the superconducting Pb film in an SRF photoinjector cavity.

II. TECHNICAL DESCRIPTION

We investigated the behavior of a Pb photocathode in the real environment of a superconducting rf gun cavity. For this purpose the lead photocathode was tested in two SRF guns, which are described in the following section.

A. SRF gun cavities with Pb cathode

In the first version of the 1.6 cell SRF gun [11,12] (called Gun 0.1) designed by DESY and Helmholtz-Zentrum Berlin (HZB) a Pb cathode with a thickness of about 200 nm and 8 mm diameter was deposited directly on the large grain Nb back wall of the gun cavity. The coating was done at the National Centre for Nuclear Research by means of filtered cathodic arc discharge at a base pressure of about 10^{-7} mbar [13]. The length of the plasma channel was about 70 cm. During the cathode deposition the gun cavity can be contaminated by dust and by deposited material, so that the cavity must be cleaned after the coating. After the film was deposited, the gun cavity was sent to JLab for buffered chemical polishing (BCP), high pressure water rinsing, and rf tests. At JLab the Pb spot was covered with a Teflon mask for BCP to reduce the size of the Pb cathode to 5 mm and to protect the Pb spot from all other treatment steps [14]. This was done to minimize the risk of quenching due to the magnetic field. The final BCP was performed with a weak solution for one minute without any protection of the Pb film. After the final treatment the gun cavity was shipped to HZB. The performance of the SRF gun cavity with the Pb cathode in the Horizontal Bi-Cavity Test (HoBiCaT) facility [15] was limited to 20 MV/m at $Q_0 = 2 \times 10^9$ [16].

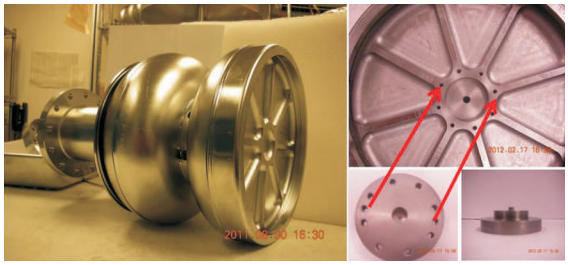

FIG. 1. Photograph of the cavity and the plug.

In the second version of the SRF gun (called Gun 0.2) a Pb cathode with a diameter of 3.5 mm and a thickness of about 400 nm was deposited on a Nb plug with a diameter of 5 mm. The distance between the Pb source and the Nb plug was about 15 cm. The coated plug can be inserted into the backplane of the cavity (see Fig. 1). For this purpose a 5 mm hole was drilled in the back wall of the cavity and the plug was vacuum sealed with an indium wire on the outside of the gun cavity. The advantage of this design is a possibility to change the photocathodes, test different deposition methods, and to make some optical measurements of the coating *ex situ* after beam operation. This concept also allows one to decouple the cavity treatment and the cathode deposition, demonstrating benefits in comparison with a direct coating on the cavity. The gun cavity with the coated plug was tested at HoBiCaT at HZB up to a peak field on the cathode of 28 MV/m at $Q_0 = 2 \times 10^9$ [16].

B. Test stand for cathode characterization

The electron beam produced in the SRF gun was characterized in the test stand [17] shown in Fig. 2, which is mounted behind the HoBiCaT cryostat. The cold system consists of the SRF gun operated at a resonance frequency of 1.3 GHz, a superconducting solenoid, and a cold steering magnet. The laser system consists of a diode-pumped Yb:YAG oscillator that generates pulses at 1030 nm wavelength, a diode-pumped regenerative amplifier, and a wavelength conversion stage that converts the infrared pulses to

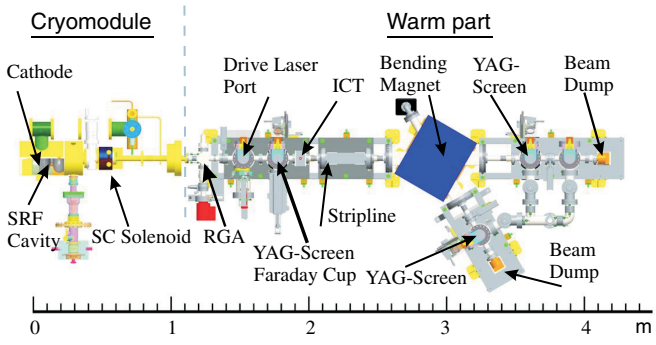

FIG. 2. Schematic view of the cold system and the beam line.

UV pulses at 258 nm. The photocathode is illuminated by UV pulses with a pulse length of 2–3 ps delivered at 8 kHz repetition rate with a pulse energy on the cathode surface of 0.03–0.2 μJ. The diagnostics beam line consists of an integrating current transformer (ICT) and a movable Faraday cup for a measurement of the average beam current and the bunch charge. The electron beam is visualized by the image of the scintillation light emitted by the cerium-doped yttrium aluminum garnet (YAG) crystal with Ce-doping concentration of 0.2% and a thickness of 100 μm. In order to avoid accumulation of the absorbed electric charge in the crystal, a thin, 10 nm, indium tin oxide coating was applied. A 60° dipole magnet is used to measure the beam momentum and the momentum spread.

C. Laser cleaning setup

The cathode can be contaminated during the cavity treatment or after the cavity is cooled down by a reaction with residual gases causing an increase of the work function and, hence, decrease of the emission current. Therefore final *in situ* cathode treatment is required after the gun cavity is cooled down. We performed laser cleaning to remove cathode contaminations. The major advantage of this method is an ability to localize the ''cleaning'' source onto the desired area, so that the gun cavity remains unaffected by this procedure. For the laser cleaning a KrF excimer laser (Xantos XS) at 248 nm ($h\nu = 5$ eV) with a FWHM pulse duration of 5–6 ns and a repetition rate of 500 Hz was used.

III. RESULTS

A. Laser cleaning in Gun 0.1

Laser cleaning of the emission surface was performed to remove the cathode contaminations in Gun 0.1. The effectiveness of the laser cleaning is mainly related to the pulse duration, wavelength, incident angle, and the absorbed energy density. During the laser cleaning the incoming energy density should be high enough to remove the contaminations from the cathode surface. On the other hand, it should be below the damage threshold of the cathode and not modify the surface morphology. In the previous work [5], it was shown that the first observable change in the surface morphology occurs at an energy density of 0.28 mJ/mm^2; therefore we performed laser cleaning with various laser energy densities, increasing stepwise from 0.045 mJ/mm^2 up to 0.23 mJ/mm^2, to minimize the risk of surface damage and sputtering of the Pb film on the cavity surface. During the laser treatment the gun cavity was cooled down to 1.8 K, but no rf power was applied.

QE maps were measured by scanning a 258 nm laser before and after each cleaning procedure at a launch phase of about 10°–15°, where the bunch is extracted from the gun completely, but the Schottky effect is still small (see Fig. 3). The laser spot was moved over the cathode surface by tilting a mirror in the laser beam line and the extracted current was measured by the Faraday cup. Prior to the laser cleaning the maximum QE of 3.6×10^{-5} was registered in the center of the photocathode (Fig. 4). For the first three laser treatments the cleaning laser was focused on the center of the photocathode with transverse FWHM size of 3.9×4.7 mm^2, so that the laser cleaning was performed without scanning the cathode surface. The surface was irradiated for 10 minutes (corresponds to 300.000 shots) for each treatment at nearly normal incident angle to the cathode surface. After the first laser cleaning with an energy density of 0.045 mJ/mm^2, the maximum QE changed by approximately 30% to 4.8×10^{-5}. At the same time an ''island'' with the same QE as in the center of the cathode occurs near the boundary between the Pb

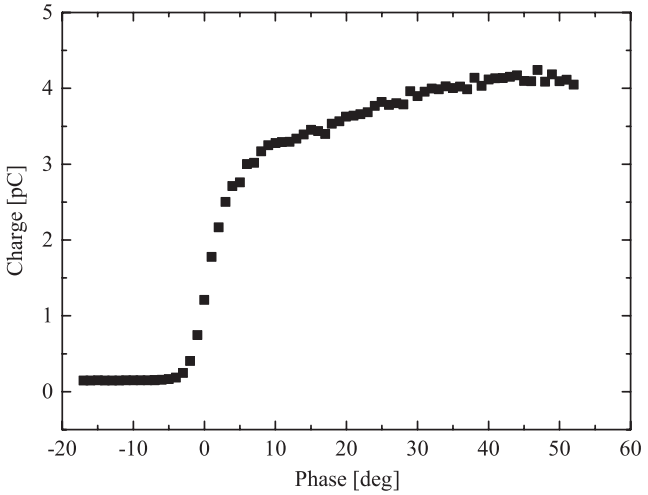

FIG. 3. Extracted charge versus launch phase at a peak field on the cathode surface of 12 MV/m.

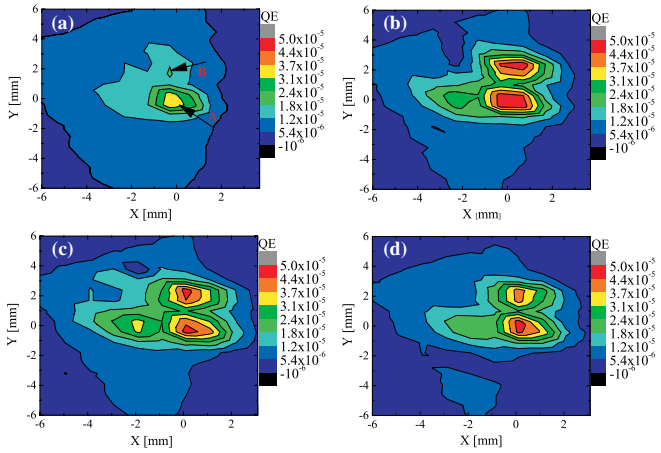

FIG. 4. QE map of Pb photocathode using 258 nm light before laser cleaning (a), and after laser cleaning with an energy density of 0.045 mJ/mm^2 (b), 0.087 mJ/mm^2 (c), and 0.09 mJ/mm^2 (d). Point (0,0) corresponds to the geometric center of the Pb spot.

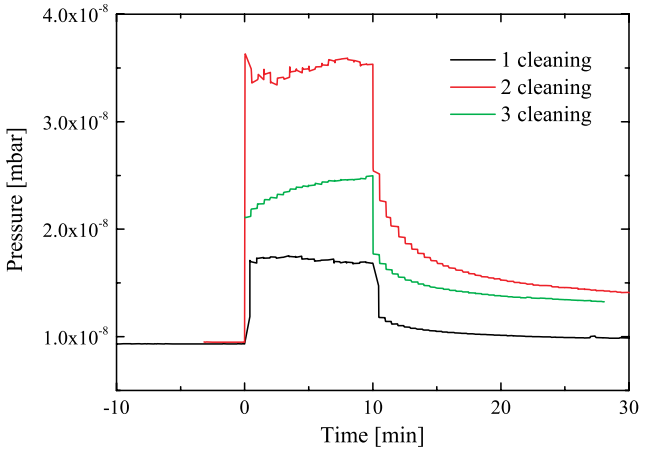

FIG. 5. Gas desorption during the laser cleaning process during the first cleaning with 0.045 mJ/mm^2, second cleaning with 0.087 mJ/mm^2, and third cleaning with 0.09 mJ/mm^2. Time "0" corresponds to the beginning of the cleaning.

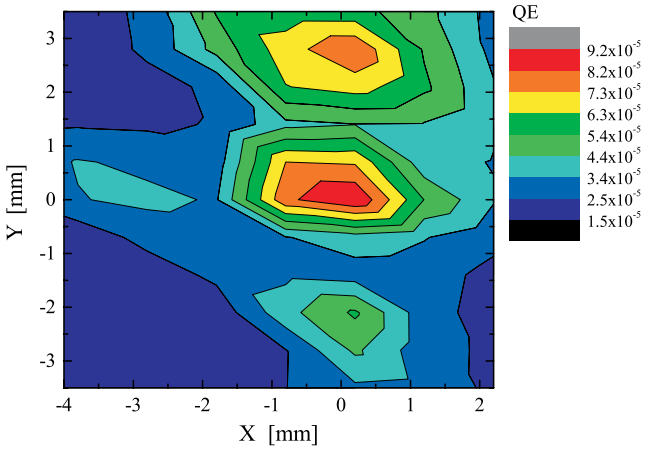

FIG. 6. Plot of QE across the surface after the final laser cleaning with an energy density of 0.23 mJ/mm^2.

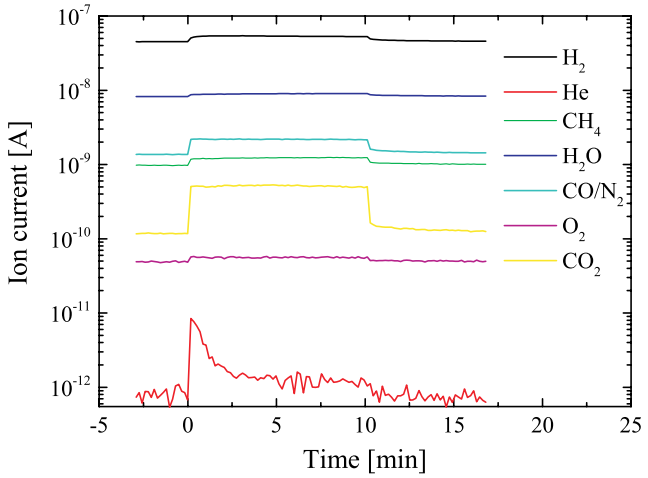

FIG. 7. Partial pressure rise during the final laser cleaning.

cathode and Nb substrate. Here an improvement of QE by a factor of 2.5 was observed. The observed inhomogeneity of the QE map after laser cleaning is not due to the nonuniform spatial profile of the cleaning laser, but probably due to the inhomogeneity of the Pb film. Laser cleaning with double laser energy of 0.087 mJ/mm^2 (performed 80 minutes after the first one) changed neither the maximum of QE nor the QE distribution significantly. The third laser cleaning was performed with the same energy density of 0.09 mJ/mm^2 to investigate whether the longer treatment influences the cathode QE.

Vacuum spectra measured by a residual gas analyzer (RGA) for the range between 1 and 100 atomic mass units, located about 1.5 m away from the cathode, was dominated by hydrogen and water. During the laser cleaning we observed a pressure rise of few 10^{-8} mbar. After the third run vacuum rise was 30% smaller than after the second one (Fig. 5).

During the final treatment the cleaning laser was focused on the cathode with transverse FWHM size of 2.3×3.5 mm^2. The laser cleaning with an energy density of 0.23 mJ/mm^2 improved the QE in the center of the cathode to 9.2×10^{-5} (Fig. 6). This value is still a factor of 5 lower than QE achieved at BNL for Pb witness samples cleaned at room temperature, but a factor of 5 higher than QE for laser cleaned Nb [5]. Additionally, there are two areas above and under the center with QE $= 8.1 \times 10^{-5}$ and QE $= 5.5 \times 10^{-5}$, respectively.

Gases desorbed during the final laser cleaning were analyzed by the residual gas analyzer. The most dominant gases in the spectrum were hydrogen, water, and carbon monoxide/nitrogen, corresponding to the masses 2, 18, and 28 (Fig. 7). During the final laser cleaning the greatest relative change of the partial pressure were due to helium, following by carbon dioxide and carbon monoxide. In contrast to all other gases the partial pressure of helium drops after about two minutes. Most of the observed gases are probably related to the molecules covering the surface during and after the cavity was cooled down, and not to the oxidized lead.

After the final laser cleaning the gun cavity was warmed up and exposed to dry nitrogen by accident. After this the cavity was again cooled down and the QE map was measured (Fig. 8). The QE in the center of the Pb spot 6×10^{-5} is still rather high, so that the maximum QE was affected only slightly by dry nitrogen.

Figure 9 presents the history of the QE at two selected points "A" and "B" on the cathode (see Fig. 4).

B. Quantum efficiency in Gun 0.2

After Gun 0.2, with the removable Pb coated plug, was installed in HoBiCaT and cooled down to 1.8 K a strong field emission was observed at a peak field on the cathode surface of 3 MV/m. A few days of rf processing were necessary to shift the onset field gradient to 28 MV/m.

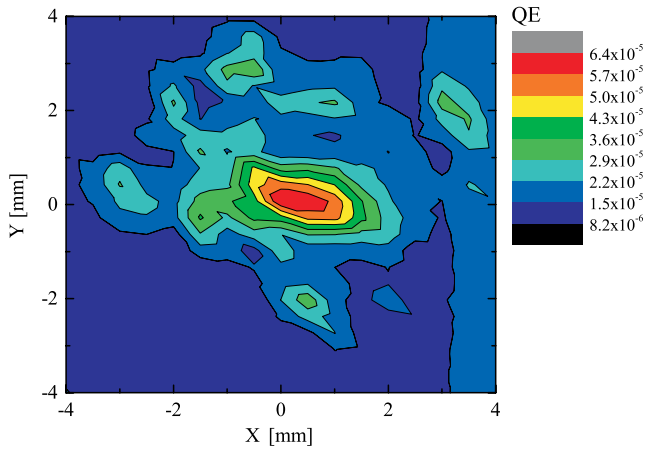

FIG. 8. QE after the cavity was vented with nitrogen.

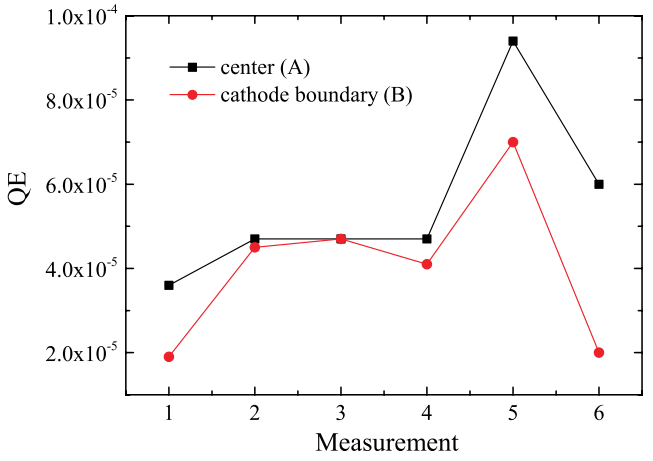

FIG. 9. History of the QE in the center (A) and near the cathode boundary (B): prior to the laser cleaning (1), after the first laser cleaning with 0.045 mJ/mm^2 (2), after the second laser cleaning with 0.087 mJ/mm^2 (3), after the third laser cleaning with 0.09 mJ/mm^2 (4), after the fourth laser cleaning with 0.23 mJ/mm^2 (5), and after the cavity was vented with dry nitrogen, warmed up and then retested (6).

Figure 10 shows the QE map of the cathode of Gun 0.2 after the rf processing. No laser cleaning was carried out in Gun 0.2 since the excimer laser used previously was not available. The maximum QE of 2×10^{-5} was measured

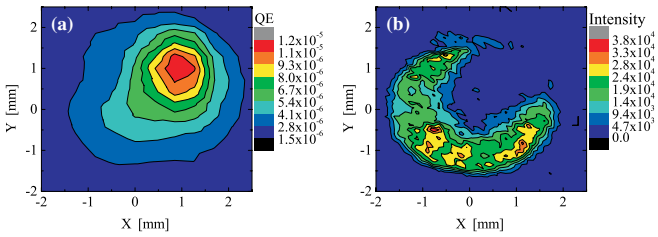

FIG. 10. QE map after rf processing (a) and luminescence map (b).

~1 mm away from the geometrical center of the coated area, which is comparable to the QE in Gun 0.1 before laser cleaning. While scanning of the back wall with the drive laser some emission was registered with the CCD camera in the visible range of the light spectrum as shown in Fig. 10. No rf power was applied during this measurement. The emitted light probably cannot be referred to the pure reflection of the drive laser, because the camera is not sensitive to the UV light ($\lambda < 400$ nm). The emitted light is most likely associated with luminescence of impurities on the cathode surface. Furthermore, it seems that QE correlates with the emitted light. Areas with higher QE have lower luminescence intensity, and the fluorescence map provides precise information about cathode impurities/contaminations.

C. Cathode work function and reflectivity

The QE of a metal cathode near the photoemission threshold can be roughly estimated as [18]

$$\mathrm{QE} \sim \frac{1-R}{1+\frac{\lambda_{\mathrm{ph}}}{\lambda_{\mathrm{ee}}}} \frac{E_{\mathrm{F}}+\hbar\omega}{2\hbar\omega}\left[1-\sqrt{\frac{E_{\mathrm{F}}+\phi_{\mathrm{eff}}}{E_{\mathrm{F}}+\hbar\omega}}\right]^2, \quad (1)$$

where R is the cathode reflectivity, λ_{ph} is the photon absorption depth, λ_{ee} is the electron-electron scattering length, E_{F} is the Fermi energy, and $\phi_{\mathrm{eff}} = \phi_0 - \phi_{\mathrm{Schottky}}$ is the cathode effective work function including work function lowering by the local electric field. The Schottky work function is given by $\phi_{\mathrm{Schottky}} = e\sqrt{\beta_{\mathrm{ph}}\frac{eE}{4\pi\varepsilon_0}}$, where β_{ph} is the field enhancement factor for photoemission (assumed to be close to 1). For a lead photocathode the electron-electron scattering length is much larger than the photon absorption length (see Table I) and Eq. (1) can be further simplified as

$$\mathrm{QE} \sim (1-R)\frac{E_{\mathrm{F}}+\hbar\omega}{2\hbar\omega}\left[1-\sqrt{\frac{E_{\mathrm{F}}+\phi_{\mathrm{eff}}}{E_{\mathrm{F}}+\hbar\omega}}\right]^2. \quad (2)$$

We measured the QE dependence on the cathode field (Fig. 11), fit the experimental data with Eq. (2), and extracted the absorption in the emitting layer $(1-R)$ and the cathode work function ϕ_0. The cathode work function $\phi_0 = 4.45$ eV is ~0.4 eV higher than the literature values

TABLE I. Pb properties at room temperature and photon wavelength of 258 nm [5,8,19,20].

Material	Pb
Reflectivity, R	0.7
Absorption length, λ_{ph}	7 nm
Electron-electron scattering length, λ_{ee}	17 nm
Work function, ϕ_0	4 eV
Fermi energy, E_{F}	9.4 eV
Melting point	600 K

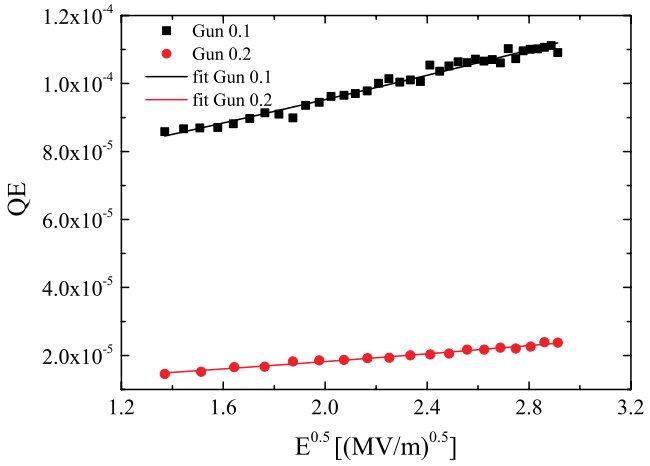

FIG. 11. QE dependence on the square root of the field gradient on the cathode surface and for Gun 0.1 (squares) and Gun 0.2 (circles). The continuous lines are the fitting curves.

[8], probably due to oxygen containing contaminations and the absorption $(1 - R) = 0.3$ in Gun 0.1. In Gun 0.2 the work function is $\phi_0 = 4.6$ eV and the absorption is $(1 - R) = 0.16$.

IV. SUMMARY

Superconducting Pb cathodes have the potential to satisfy the requirements of FEL's and deliver an electron beam with high peak and medium average current. The key challenge is to remove the cathode contaminations after the cavity treatment and to get a homogeneous QE distribution over the entire cathode surface without changing the cavity performance. For an SRF gun with Pb cathode it is absolutely necessary to implement some appropriate cathode cleaning techniques. The maximum QE value of 9×10^{-5} at 258 nm was achieved in Gun 0.1 after the laser cleaning with energy density of 0.23 mJ/mm^2. This value achieved within the cryogenic environment is a factor of 5 lower than QE measured at BNL on Pb witness samples without BCP or other treatment steps typical for the cavities, but a factor of 5 higher than QE for laser cleaned Nb. To get a more homogeneous distribution of QE more attention should be paid to the cavity treatment and laser cleaning with a smaller homogeneous spot scanning across the cathode. For a possible CW upgrade of the European XFEL facility the electron source must deliver 0.1 nC bunches separated by 4 μs. For a lead photocathode with a demonstrated QE of 9×10^{-5} the UV laser must provide an average power of 1.3 W and an energy of 5.3 μJ per pulse on the cathode surface. For a possible long pulse upgrade of the XFEL the electron source must deliver 100 ms long pulses separated by 1 Hz. Within the macropulse the bunch repetition rate is 250 kHz at a bunch charge of 0.5 nC. For this scenario the drive laser must provide an average power of 0.7 W and a pulse energy of 26.7 μJ on the cathode surface. Such laser parameters are feasible with the present state-of-the-art laser systems.

ACKNOWLEDGMENTS

The authors acknowledge fruitful discussions with K. Aulenbacher, D. Dowell, and V. I. Shvedunov. We would also like to thank M. Schenk for technical support. This work was supported by Bundesministerium für Bildung und Forschung and Land Berlin. The Pb deposition activity is supported by EuCARD.

[1] J. Sekutowicz, *Multi-cell Superconducting Structures for High Energy e^+e^- Colliders and Free Electron Laser Linacs*, edited by R. Romaniuk (Publishing House of Warsaw University of Technology, Warsaw, 2008) [https://eucard.web.cern.ch/EuCARD/activities/communication/booklets].

[2] A. Arnold, H. Büttig, D. Janssen, T. Kamps, G. Klemz, W. D. Lehmann, U. Lehnert, D. Lipka, F. Marhauser, P. Michel, K. Möller, P. Murcek, Ch. Schneider, R. Schurig, F. Staufenbiel, J. Stephan, J. Teichert, V. Volkov, I. Will, and R. Xiang, Nucl. Instrum. Methods Phys. Res., Sect. A **577**, 440 (2007).

[3] T. Rao, I. Ben-Zvi, A. Burrill, H. Hahn, D. Kayran, Y. Zhao, P. Kneisel, and M. Cole, in *Proceedings of the 2005 Particle Accelerator Conference, Knoxville, Tennessee, USA, 2005*, edited by C. Horak (IEEE, Piscataway, NJ, 2005) p. 2556.

[4] D. E. Eastman, Phys. Rev. B **2**, 1 (1970).

[5] J. Smedley, T. Rao, and J. Sekutowicz, Phys. Rev. ST Accel. Beams **11**, 013502 (2008).

[6] J. Sekutowicz, S. A. Bogacz, D. Douglas, P. Kneisel, G. P. Williams, M. Ferrario, I. Ben-Zvi, J. Rose, J. Smedley, T. Srinivasan-Rao, L. Serafini, W.-D. Möller, B. Petersen, D. Proch, S. Simrock, P. Colestock, and J. B. Rosenzweig, Phys. Rev. ST Accel. Beams **8**, 010701 (2005).

[7] A. C. Rose-Innes and E. H. Rhoderick, *Introduction to Superconductivity*, International Series in Solid State Physics (Pergamon Press, New York, 1978), 2nd ed.

[8] N. D. Lang and W. Kohn, Phys. Rev. B **3**, 1215 (1971).

[9] F. Zhou, A. Brachmann, F.-J. Decker, P. Emma, S. Gilevich, R. Iverson, P. Stefan, and J. Turner, Phys. Rev. ST Accel. Beams **15**, 090703 (2012).

[10] A. Lorusso, F. Gontad, A. Perrone, and N. Stankova, Phys. Rev. ST Accel. Beams **14**, 090401 (2011).

[11] T. Kamps, W. Anders, R. Barday, A. Jankowiak, J. Knobloch, O. Kugeler, A. Matveenko, A. Neumann, T. Quast, J. Rudolph, S. Schubert, J. Völker, P. Kneisel, R. Nietubyc, J. Sekutowicz, J. Smedley, V. Volkov, G. Weinberg, and I. Will, in *Proceedings of the 2nd International Particle Accelerator Conference, San Sebastian, Spain, 2011* (EPS-AG, Spain, 2011), p. 3143.

[12] A. Neumann, W. Anders, R. Barday, A. Jankowiak, T. Kamps, J. Knobloch, O. Kugeler, A. Matveenko, T. Quast, J. Rudolph, S. Schubert, J. Völker, J. Smedley, J. Sekutowicz, P. Kneisel, R. Nietubyc, I. Will, and G. Lorenz, in Proceedings of the 15th International

Conference on RF Superconductivity, Chicago, USA, 2011 , p. 962.

[13] P. Strzyzewski, J. Langner, M. Sadowski, J. Witkowski, S. Tazzari, R. Russo, J. Sekutowicz, T. Rao, and J. Smedley, in *Proceedings of the 10th European Particle Accelerator Conference, Edinburgh, UK, 2006*, edited by C. Biscari (EPS-AG, Edinburgh, Scotland, 2006), p. 3209.

[14] P. Kneisel, J. Sekutowicz, R. Nietubyc, O. Kugeler, A. Neumann, T. Kamps, and J. Knobloch, in *Proceedings of the 2011 Particle Accelerator Conference, New York, NY, USA, 2011* (IEEE, New York, 2011), p. 1047.

[15] O. Kugeler, A. Neumann, W. Anders, and J. Knobloch, Rev. Sci. Instrum. **81**, 074701 (2010).

[16] A. Burrill, W. Anders, T. Kamps, J. Knobloch, O. Kugeler, P. Lauinger, A. Neumann, J. Sekutowicz, P. Kneisel, and R. Nietubyc, in Proceedings of the 2013 International Particle Accelerator Conference, Shanghai, China, 2013 (JACoW, 2013), p. 2313.

[17] R. Barday, A. Jankowiak, T. Kamps, A. Matveenko, M. Schenk, F. Siewert, J. Völker, and J. Teichert, in Proceedings of the 1st International Beam Instrumentation Conference, Tsukuba, Japan, 2012 (JACoW, 2012), p. 241.

[18] D. H. Dowell and J. F. Schmerge, Phys. Rev. ST Accel. Beams **12**, 074201 (2009).

[19] J. C. Lemonnier, M. Priol, and S. Robin, Phys. Rev. B **8**, 5452 (1973).

[20] *CRC Handbook of Chemistry and Physics*, edited by D. R. Lide (CRC Press, Boca Raton, FL, 2003), 84th ed.